

LIGO Laboratory / LIGO Scientific Collaboration

LIGO-T050066-03-D

Advanced LIGO

6/16/05

**Beamsplitter
Diffraction Loss
(Advanced LIGO)**

Michael Smith

Distribution of this document:
LIGO Science Collaboration

This is an internal working note
of the LIGO Project.

California Institute of Technology
LIGO Project – MS 18-34
1200 E. California Blvd.
Pasadena, CA 91125
Phone (626) 395-2129
Fax (626) 304-9834
E-mail: info@ligo.caltech.edu

Massachusetts Institute of Technology
LIGO Project – NW17-161
175 Albany St
Cambridge, MA 02139
Phone (617) 253-4824
Fax (617) 253-7014
E-mail: info@ligo.mit.edu

LIGO Hanford Observatory
P.O. Box 1970
Mail Stop S9-02
Richland WA 99352
Phone 509-372-8106
Fax 509-372-8137

LIGO Livingston Observatory
P.O. Box 940
Livingston, LA 70754
Phone 225-686-3100
Fax 225-686-7189

<http://www.ligo.caltech.edu/>

Table of Contents

1 Introduction **5**

1.1 Scope **5**

1.2 Referenced Documents **5**

2 Analysis **6**

2.1 Beam Size at the ITM **6**

2.2 Beam Size at the BS **6**

 2.2.1 No Lensing at RAM 6

 2.2.2 Lens at RAM 7

2.3 Optimum Position of Input Beam on BS HR Surface **7**

 2.3.1 Optimum Input Beam Displacement at the BS HR 7

 2.3.2 Lateral Displacement of Beam Through BS AR 8

3 Results **10**

3.1 Baseline BS **10**

 3.1.1 Input Gaussian Beam 10

 3.1.2 Input Beam through Power Recycling Mirror, No Bonding Flats 11

 3.1.3 Input Beam through Signal Recycling Mirror, No Bonding Flats 17

 3.1.4 Loss as a Function of BS Thickness and Diameter, No Bonding Flats 24

 3.1.5 Loss as a Function of Bonding Flat Length 28

3.2 Alternative Design with Lens at RAM **31**

 3.2.1 RAM Lens Configuration 31

 3.2.2 BS Power Loss with RAM Lens 32

 3.2.3 Beam Steering with RAM Lens 35

4 Conclusions **36**

4.1 Standard Configuration: No Lensing at RAM **36**

4.2 Alternate Configuration: 9000 mm Radius on Back Surface of RAM **36**

 4.2.1 Potential Problems with Lens at RAM 37

4.3 Power Loss Due to Bonding Flats **37**

Table of Tables

Table 1 : BS Loss Comparison for Two Configurations **36**

Table 2: Alternative Design, BS Loss Comparison for Two Configurations..... **36**

Table of Figures

Figure 1: BS Geometry..... **7**

Figure 2: Optimum offset of Input Beam.....	8
Figure 3: Lateral Displacement of Refracted Beam through BS.....	9
Figure 4: Input Gaussian Beam.....	10
Figure 5: Optical Schematic, Power Recycling Input Transmission through BS	11
Figure 6: X-cross Section at ITMx HR, PR Input, Transmitted Arm.....	11
Figure 7: Y-cross Section at ITMx HR, PR Input, Transmitted Arm.....	12
Figure 8: X-cross Section of Diffracted Beam around ETMx, PR Input, Transmitted Arm.....	13
Figure 9: Y-cross Section of Diffracted Beam around ETMx, PR Input, Transmitted Arm.....	13
Figure 10: Optical Schematic, Power Recycling Input Reflection from BS 50:50 Surface	14
Figure 11: X-cross Section at ITMy HR, PR Input, Reflected Arm.....	15
Figure 12: Y-cross Section at ITMy HR, PR Input, Reflected Arm	15
Figure 13: X-cross Section of Diffracted Beam around ETMy, PR Input, Reflected Arm	16
Figure 14: Y-cross Section of Diffracted Beam around ETMy, PR Input, Reflected Arm	17
Figure 15: Optical Schematic, Signal Recycling Input Reflection from BS 50:50 Surface.....	17
Figure 16: X-cross Section at ITMx HR, SR Input, Transmitted Arm.....	18
Figure 17: Y-cross Section at ITMx HR, SR Input, Transmitted Arm	19
Figure 18: X-cross Section of Diffracted Beam around ETMx, SR Input, Transmitted Arm.....	20
Figure 19: Y-cross Section of Beam around ETMx, SR Input, Transmitted Arm.....	20
Figure 20: Optical Schematic, Signal Recycling Input Transmission through BS 50:50 Surface ...	21
Figure 21: X-cross Section at ITMy HR, SR Input, Reflected Arm	22
Figure 22: Y-cross Section at ITMy HR, SR Input, Reflected Arm.....	22
Figure 23: X-cross Section of Diffracted Beam around ETMy, SR Input, Reflected Arm.....	23
Figure 24: Y-cross Section of Diffracted Beam around ETMy, SR Input, Reflected Arm.....	24
Figure 25: BS Total Loss Transmitted arm, PR Input.....	25
Figure 26: BS Total Loss Reflected arm, PR Input	25
Figure 27: BS Total Loss Both Arms, PR Input.....	26
Figure 28: BS Total Loss Transmitted Arm, SR Input	26
Figure 29: BS Total Loss Reflected Arm, SR Input	27
Figure 30: BS Total Loss Both Arms, SR Input.....	27
Figure 31: Bonding Flat Geometry	28
Figure 32: Power Loss in Transmitted Arm, SR Input with Flats	29
Figure 33: Power Loss in Reflected Arm, SR Input with Flats.....	29
Figure 34: Power Loss in Both Arms, SR Input with Flats	30
Figure 35: Power Loss in Transmitted Arm, PR Input with Flats.....	30
Figure 36: Power Loss in Reflected Arm, PR Input with Flats	31
Figure 37: Power Loss in Both Arms, PR Input with Flats.....	31
Figure 38: Optical Schematic, Alternative Design with Lens in RAM.....	32
Figure 39: BS Total Loss Transmitted arm, PR Input with RAM lens	32
Figure 40: BS Total Loss Reflected arm, PR Input with RAM lens.....	33
Figure 41: BS Total Loss Both Arms, PR Input with RAM lens	33
Figure 42: BS Total Loss Transmitted Arm, SR Input with RAM lens.....	34
Figure 43: BS Total Loss Reflected Arm, SR Input with RAM lens	34
Figure 44: BS Total Loss Both Arms, SR Input with RAM lens	35
Figure 45: Beam Steering by RAM Lens.....	35

Abstract

The geometric and diffractive optical power losses of the input beam from the power recycling (PR) and signal recycling (SR) mirror directions were calculated as a function of the diameter and thickness of the beamsplitter for Adv LIGO, using the ZEMAX physical optics propagation analysis.

Two configurations were considered: 1) the standard configuration, which includes the proposed BS dimension of $t = 60$ mm, $D = 370$ mm, and 2) an alternative configuration, in which a lens element was incorporated into the ITM reaction mass (RAM) for reducing the spot size at the BS.

With the proposed BS dimensions and no lensing in the RAM, the total power loss for both arms with the PR input beam is 1.61 E-4 ; the total power loss for both arms with the SR input beam is 4.18 E-4 .

With the alternate configuration incorporating a 9000 mm radius of curvature on the back surface of the RAM, comparable total power loss occurs for a BS size of $t = 40$ mm, $D = 270$ mm, which is similar to the size used for initial LIGO.

With a BS size of $t = 60$ mm and $D = 370$ mm, bonding flats up to 100 mm long result in a total power loss in both arms of less than 0.1%.

1 Introduction

One of the factors that must be considered in choosing the dimensions for the beamsplitter for advanced LIGO is the geometric optical power loss caused by the finite diameter of the tilted beamsplitter, including bonding flats, and the diffraction losses around the edges of the beamsplitter.

1.1 Scope

This technical note will summarize the results of the physical optics propagation analysis. ZEMAX optical design program was used to calculate the geometric and diffractive optical power losses of the input beam from the power recycling (PR) and signal recycling (SR) mirror directions as a function of the diameter and thickness of the beamsplitter in Adv LIGO. The losses due to bonding flats on the BS were also calculated.

An alternative vertex configuration is considered in which a lens element was added to the ITM reaction mass (RAM). This reduces the spot size at the beam splitter (BS) and allows a smaller diameter BS to be used for the same power loss.

1.2 Referenced Documents

ZEMAX Optical Design Program User's Guide, April 9, 2005 Zemax Development Corporation
Garilynn. Billingsley, Specification for Advanced LIGO COC, LIGO-T000140-00, 11/15/00 (rev 12/3/04)

2 Analysis

The Gaussian beam incident on the beam splitter (BS) of the LIGO interferometer is vignetted by the finite size and the 45 deg orientation of the BS, resulting in a geometric loss of beam power incident on the input test mass (ITM). The edges of the BS and the edges of the ITM produce edge diffraction, which result in additional losses of beam power during traversal to the end test mass (ETM).

The input beam incident on the BS from the power recycling (PR) mirror can be offset laterally so that the input beam centerline passes through the geometric center of the BS at the internal mid-plane of the BS. This offset minimizes the transmission loss through the BS.

However, it may be better to center the input beam from the PR mirror onto the BS HR surface because that minimizes the power loss from the signal recycling (SR) mirror direction. The geometric and diffractive losses of the beam input into the interferometer from the signal recycling mirror are larger than the losses experienced by the main beam input through the power recycling mirror because of the lateral offset of the beams exiting the BS AR surface.

The geometric and diffractive losses with the input beam centered on the HR surface of the BS were calculated using physical optics propagation analysis of the ZEMAX Optical Design Program. The ZEMAX physical optics propagation analysis calculates the amplitude and phase of wave fronts propagated through the optical system using Fresnel diffraction theory of a scalar field. This approach is accurate except in optical systems that have very low f-numbers on the order of 1. The results are dependent upon the sampling size chosen for the analysis. With the 256 x 256 sampling array chosen for these current calculations, the results are expected to be accurate within 10%.

2.1 Beam Size at the ITM

The beam size at the ITM was taken to be 60mm. The baseline arm cavity design has ITM and ETM mirrors with radii of curvature 2076m separated by a cavity length of 4000m. The 11.49 mm beam waist occurs in the middle of the arm cavity 2000m away from the ITM. The relation between the beam size at the ITM and the beam waist is described by the following Gaussian beam propagation equation.

$$w_{\text{bs}} := w_0 \cdot \left[1 + \left(\frac{\lambda \cdot z}{\pi \cdot w_0^2} \right)^2 \right]^{0.5}$$

2.2 Beam Size at the BS

2.2.1 No Lensing at RAM

With no lensing at the RAM, the beam size at the BS is approximately the same as the beam size at the ITM, which is 60mm.

2.2.2 Lens at RAM

With a 9000mm radius placed on the RAM back surface, the plano-convex lens that is formed reduces the beam size at the BS to 46.8 mm.

2.3 Optimum Position of Input Beam on BS HR Surface

The geometry of the BS and the four reflected and refracted beams are shown in Figure 1.

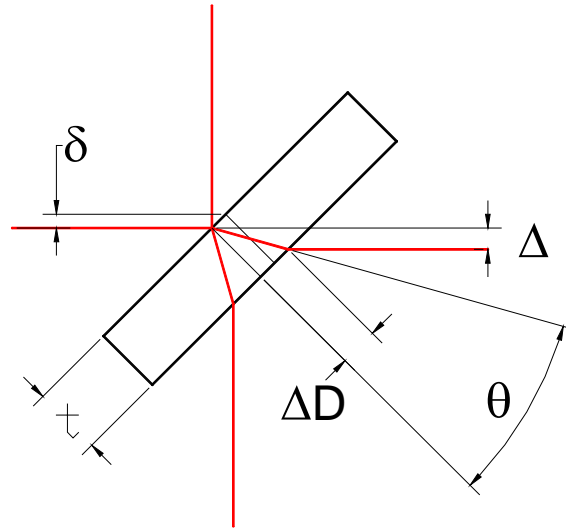


Figure 1: BS Geometry

The refraction angle at the BS HR surface is given by the following equation.

$$\theta := \text{asin}\left(\frac{\sin\left(\frac{\pi}{4}\right)}{n}\right)$$

where $n = 1.449636$ is the index of refraction of fused silica (SUPRASIL).

The displacement of the refracted input beam as it emerges from the AR surface of the BS is given by the following equation.

$$\Delta D(t) := t \cdot \tan(\theta)$$

2.3.1 Optimum Input Beam Displacement at the BS HR

2.3.1.1 Maximum Transmission through BS, PR input

Maximum transmission through the BS, when the input is from the direction of the power recycling mirror (PR), occurs when the input beam is displacement laterally by the amount

$$\delta(t) := \frac{\Delta D(t)}{2} \cdot \cos\left(\frac{\pi}{4}\right)$$

The optimum lateral displacement depends only upon the thickness of the BS and is shown in Figure 2 for various thicknesses.

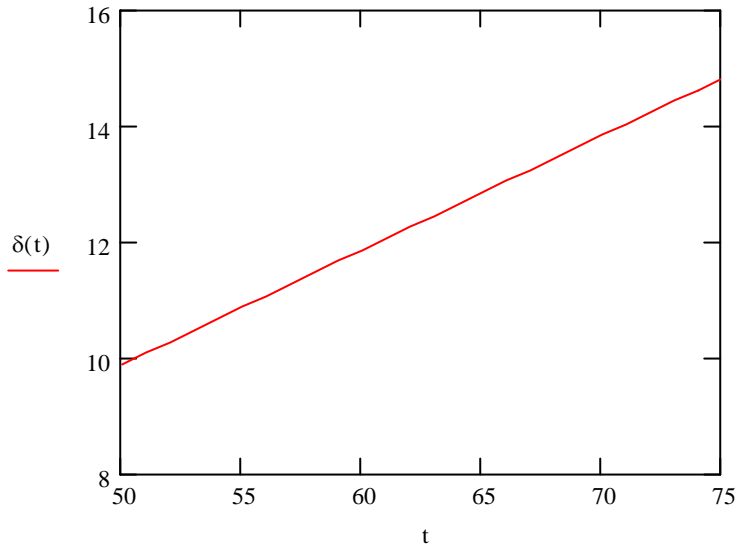


Figure 2: Optimum offset of Input Beam for max power with PR input

2.3.1.2 Maximum Transmission through BS, SR input

Maximum transmission through the BS into the transmitted arm is obtained when the input beam from the signal recycling mirror (SM) is displaced laterally by the amount

$$\Delta y_t(t) := \Delta D(t) \cdot \cos\left(\frac{\pi}{4}\right)$$

In this case, the input beam from the PR direction is centered on the BS HR surface. This seems to be the preferred orientation of both the PR and SR beams for balancing the power in both arms.

2.3.2 Lateral Displacement of Beam Through BS AR

The refracted beam transmitted through the AR surface of the BS undergoes a lateral displacement given by the following equation, which depends only upon the thickness of the BS and the fixed diffraction angle.

$$\Delta(t) := \frac{t \cdot \sin\left(\frac{\pi}{4} - \theta\right)}{\cos(\theta)}$$

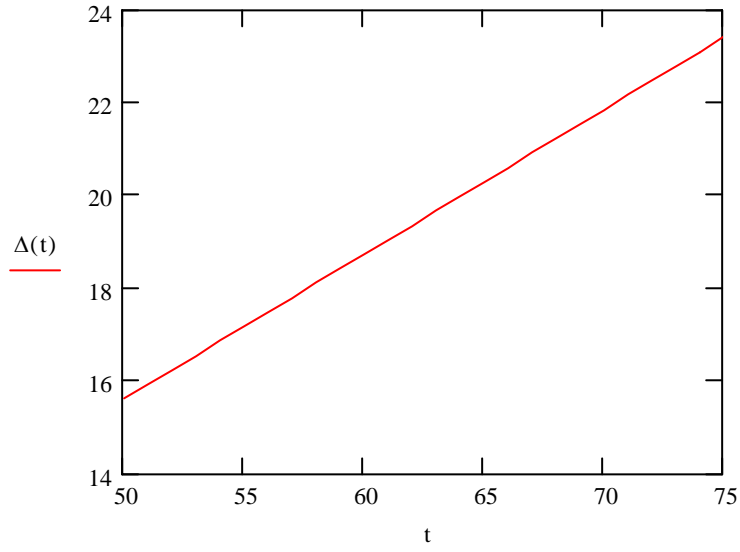


Figure 3: Lateral Displacement of Refracted Beam through BS

3 Results

The following results were calculated with the input beam from the PR mirror centered on the BS HR surface. This minimizes the loss of the beam input from the SR mirror direction. The input power is 1 W, and the BS HR reflectivity is 50%. The total loss from both arms is the sum of the individual arm losses.

3.1 Baseline BS

The Advanced LIGO baseline dimensions for the BS are:

$$t = 60 \text{ mm}$$

$$D = 350 \text{ mm}$$

3.1.1 Input Gaussian Beam

The input Gaussian beam cross section from the power recycling mirror, at the BS HR surface, is shown in Figure 4. The spot size at the BS is 60mm. The beam has a waist of 11.49 mm inside the IFO arm at a distance $z = 2005000$ mm.

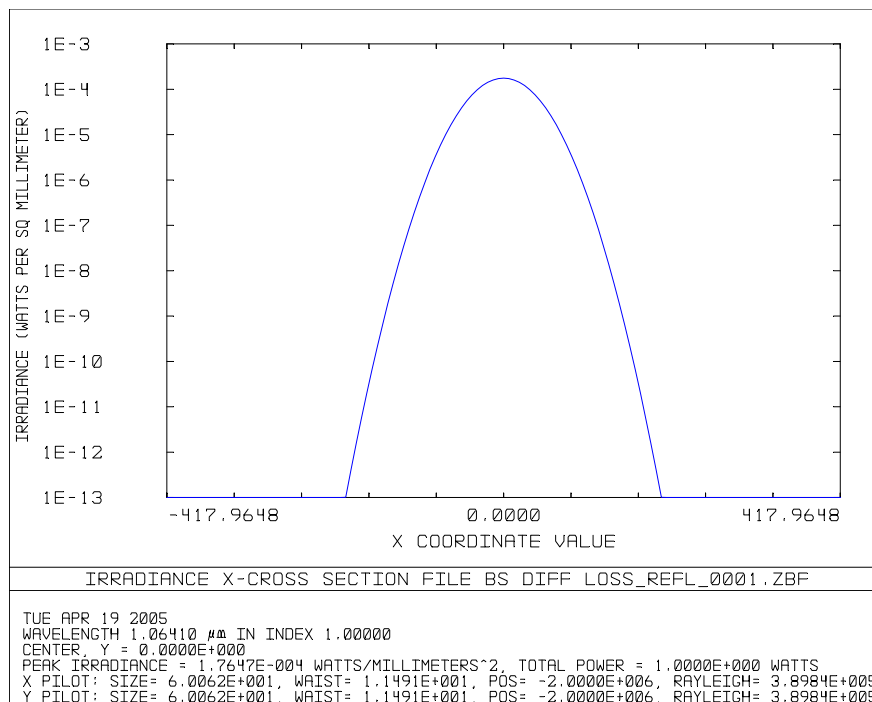


Figure 4: Input Gaussian Beam

3.1.2 Input Beam through Power Recycling Mirror, No Bonding Flats

3.1.2.1 Transmitted Arm

An optical schematic of the transmitted beam path from the power recycling mirror (PR), through the BS, through the RAM, through the ITM_x, and out to the ETM_x is shown in Figure 5.

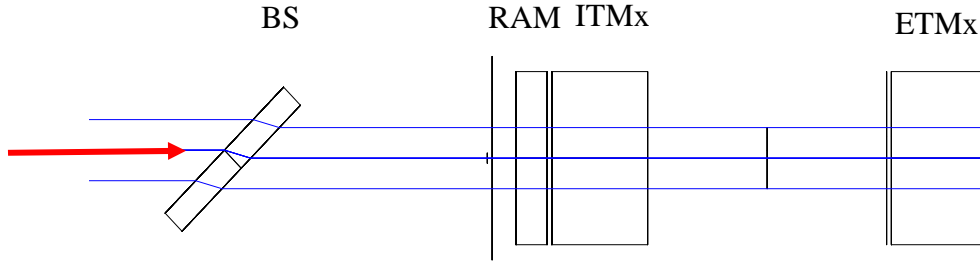


Figure 5: Optical Schematic, Power Recycling Input Transmission through BS

3.1.2.1.1 Beam Cross-section at HR surface of ITM_x, PR input, Transmitted Arm

The x (vertical) and y (horizontal) beam cross sections at a location immediately behind the ITM_x are shown in Figure 6 and Figure 7 respectively. Note that the y beam cross section is vignetted by a greater amount than the x beam cross section because of the tilted BS.

The geometric power loss after traversing through the BS is 2.92E-4 W.

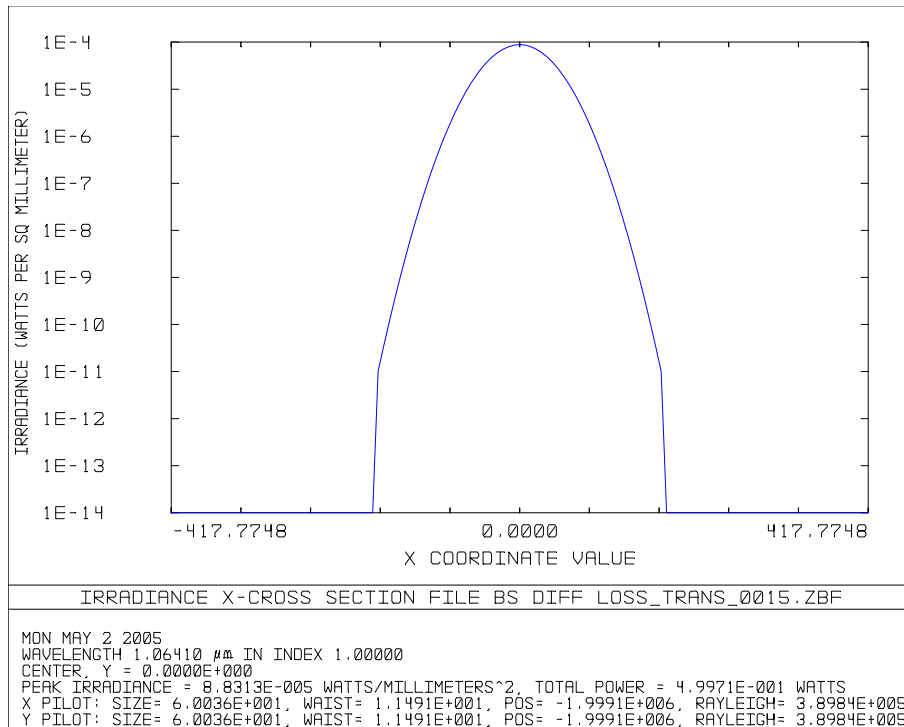


Figure 6: X-cross Section at ITM_x HR, PR Input, Transmitted Arm

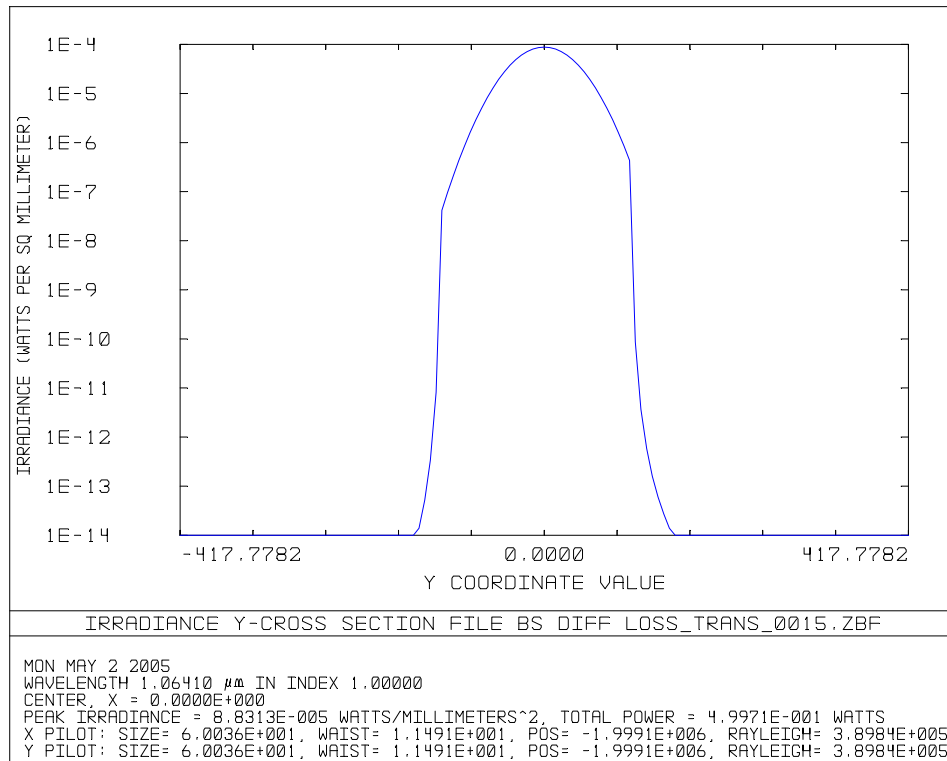


Figure 7: Y-cross Section at ITMx HR, PR Input, Transmitted Arm

3.1.2.1.2 Diffracted Power Loss around ETMx

The vignetted beam exhibits edge diffraction around the edges of the BS and the ITM. The diffracted beam is lost around the edges of the ETM, as shown in Figure 8 and Figure 9. Note that the lost diffracted power is greater in the y cross section.

The diffractive power loss at the ETMx is $6.00\text{E-}5$ W, approximately 21% of the geometric loss.

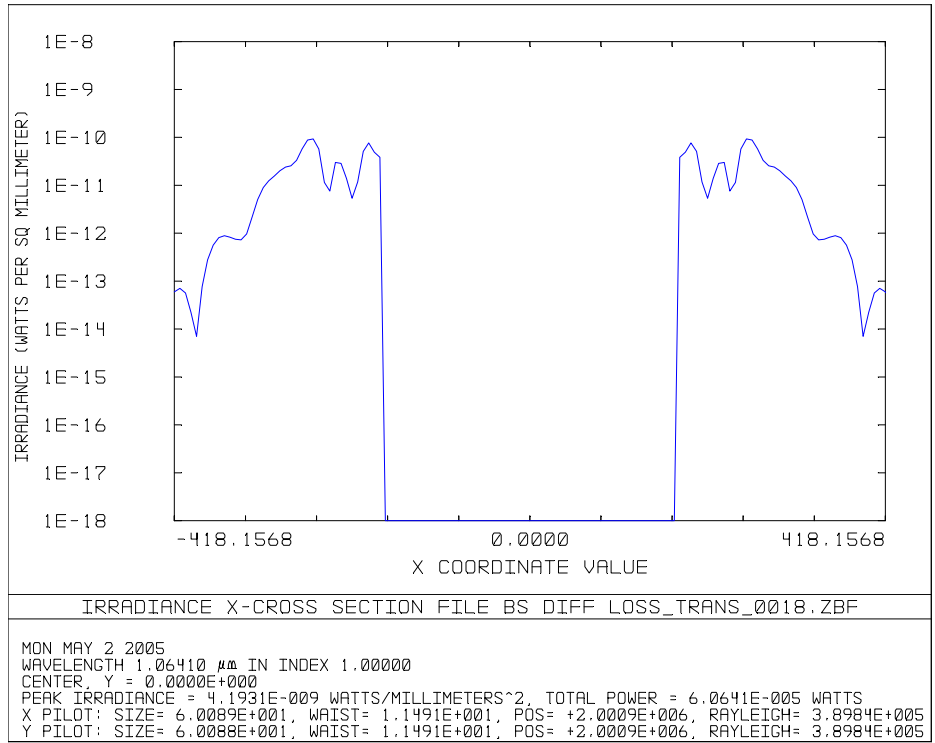


Figure 8: X-cross Section of Diffracted Beam around ETMx, PR Input, Transmitted Arm

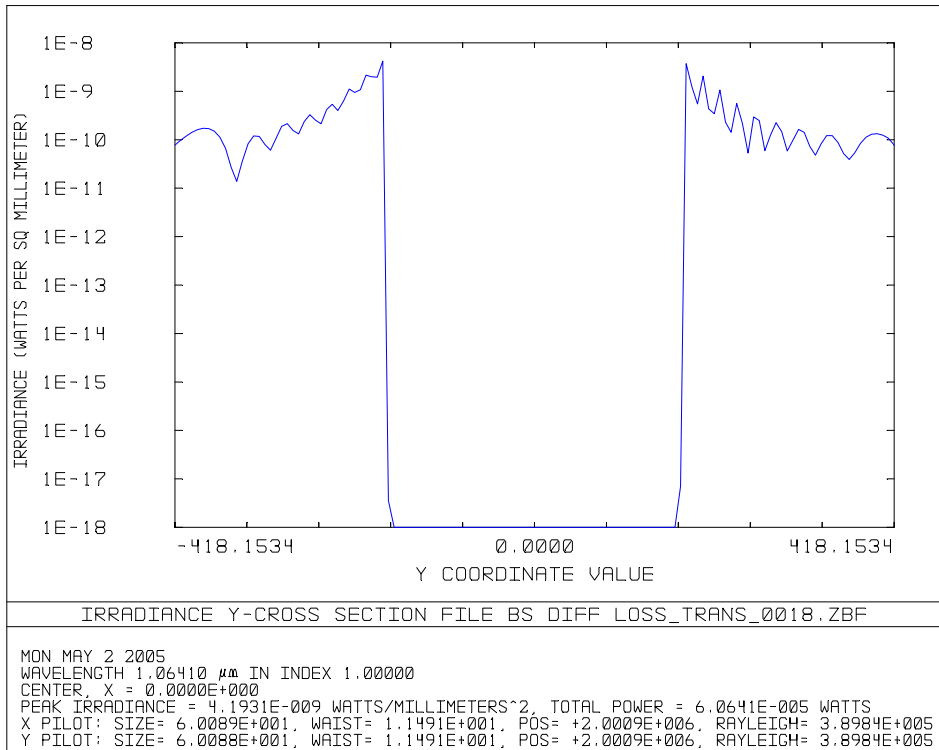


Figure 9: Y-cross Section of Diffracted Beam around ETMx, PR Input, Transmitted Arm

3.1.2.2 Reflected Arm

An optical schematic of the reflected beam path from the power recycling mirror (PR), reflecting from the HR surface of the BS, through the ITMy, and out to the ETMy is shown in Figure 10.

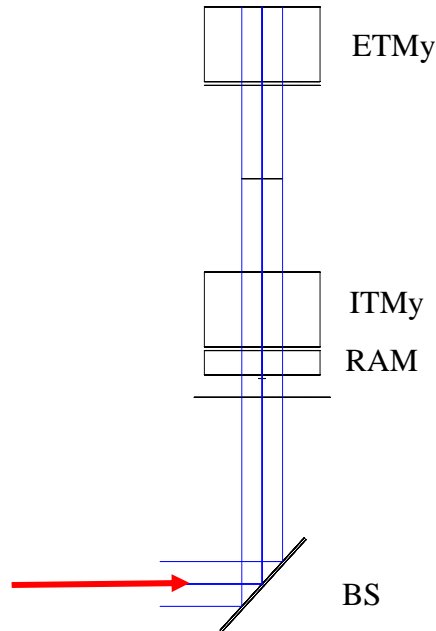


Figure 10: Optical Schematic, Power Recycling Input Reflection from BS 50:50 Surface

3.1.2.2.1 Beam Cross-section at HR surface of ITMy, PR input, Reflected Arm

The x (vertical) and y (horizontal) beam cross sections at a location immediately behind the ITMy are shown in Figure 11 and Figure 12 respectively. Note that the y beam cross section is vignettted by a greater amount than the vertical beam cross section because of the tilted BS.

The geometric power loss after reflecting from the BS is $3.2E-5$ W.

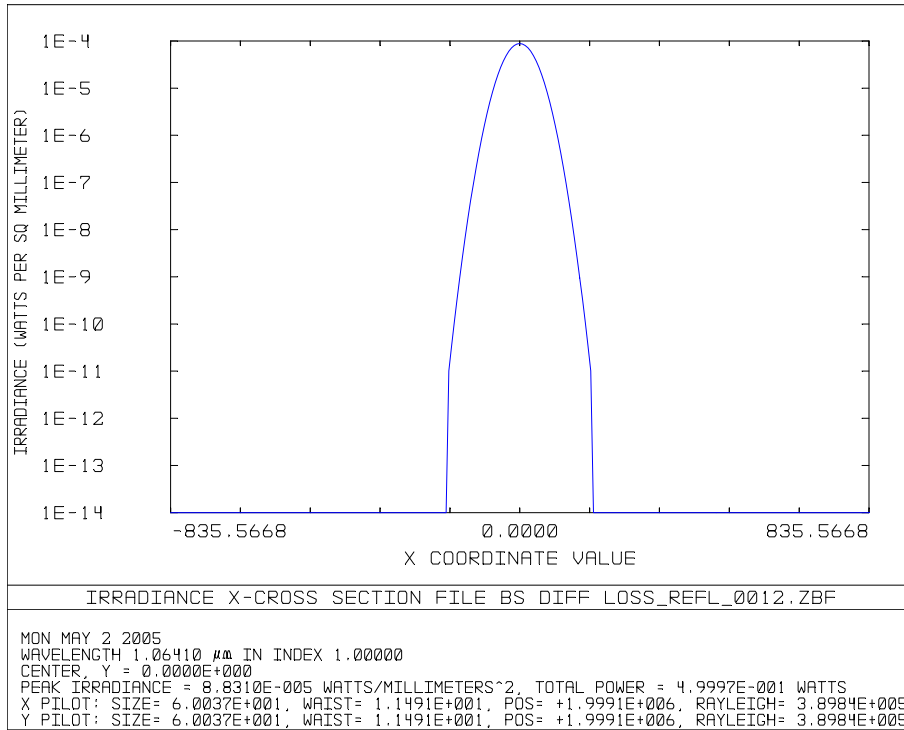


Figure 11: X-cross Section at ITMy HR, PR Input, Reflected Arm

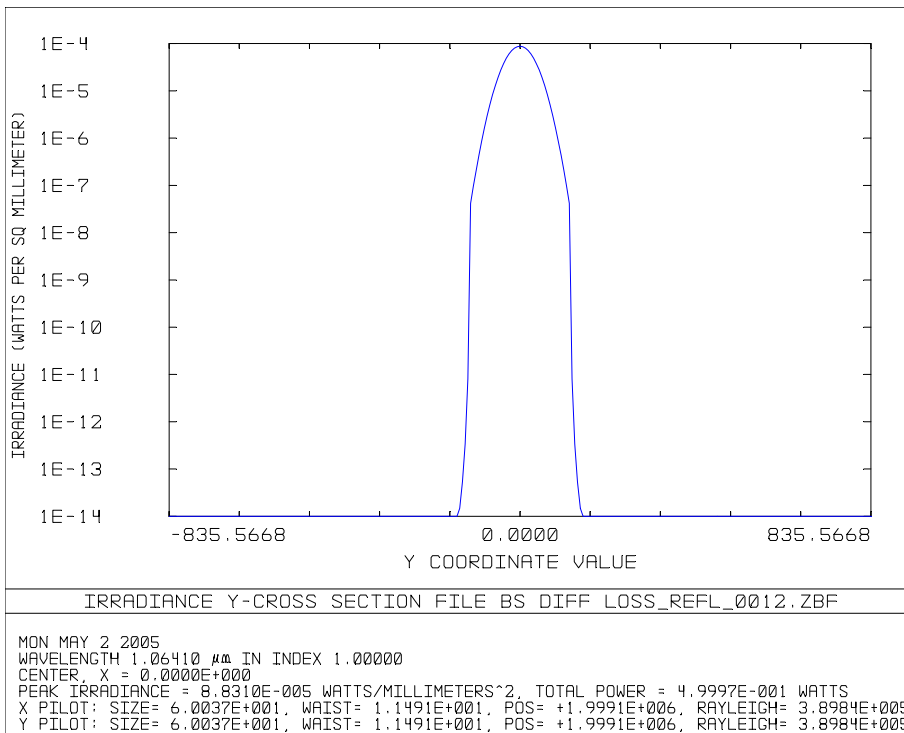


Figure 12: Y-cross Section at ITMy HR, PR Input, Reflected Arm

3.1.2.2.2 Diffracted Power Loss around ETMy

The vignetted beam exhibits edge diffraction around the edges of the BS and the ITM. The diffracted beam is lost around the edges of the ETM, as shown in Figure 13 and Figure 14. Note that the lost diffracted power is greater in the y cross section.

The diffractive power loss at the ETMy is $1.00\text{E-}5$ W, approximately 31% of the geometric loss.

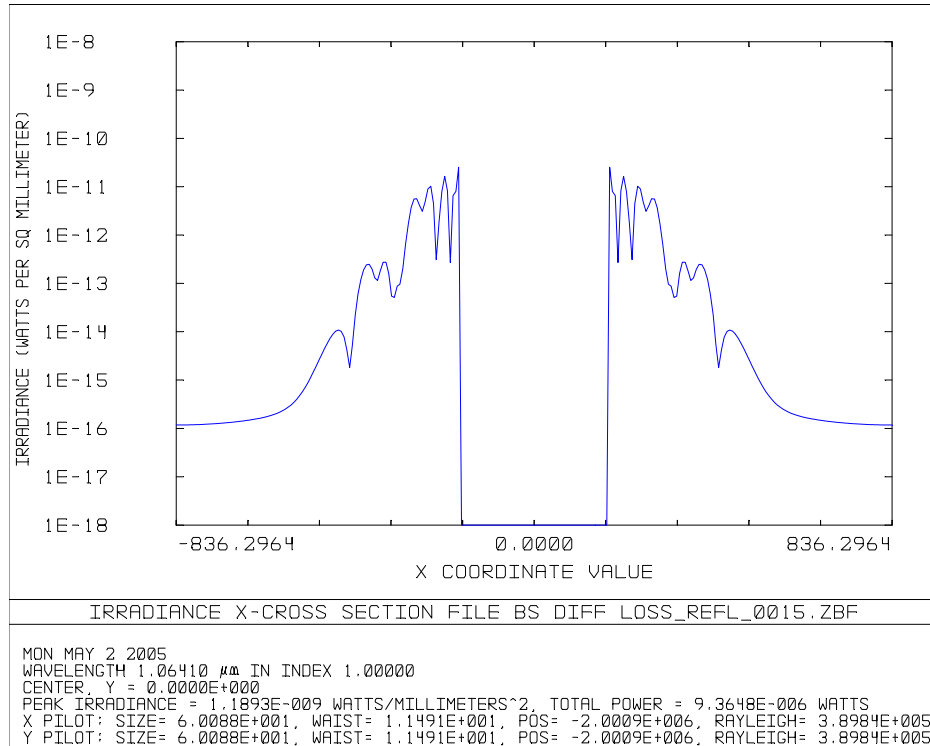


Figure 13: X-cross Section of Diffracted Beam around ETMy, PR Input, Reflected Arm

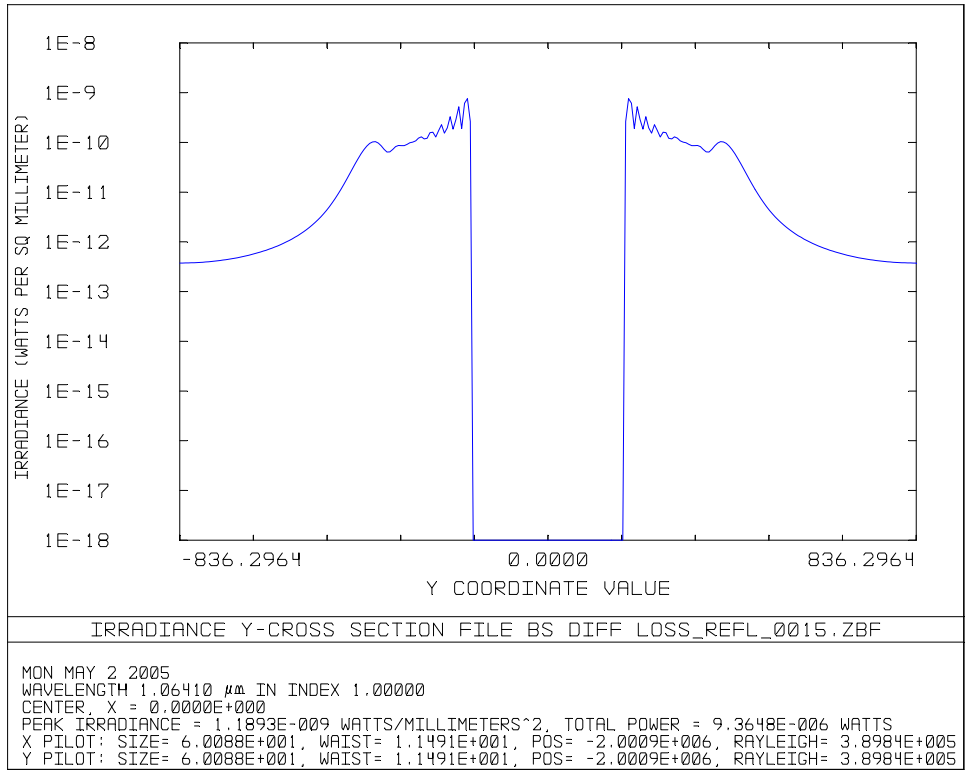


Figure 14: Y-cross Section of Diffracted Beam around ETMy, PR Input, Reflected Arm

The combined geometric and diffractive loss for both arms with PR input is 3.94E-4 W.

3.1.3 Input Beam through Signal Recycling Mirror, No Bonding Flats

3.1.3.1 Transmitted Arm

An optical schematic of the transmitted arm beam path with input from the signal recycling mirror (SR), reflecting from the HR surface of the BS, through the RAM, through the ITM_x, and out to the ETM_x is shown in Figure 15.

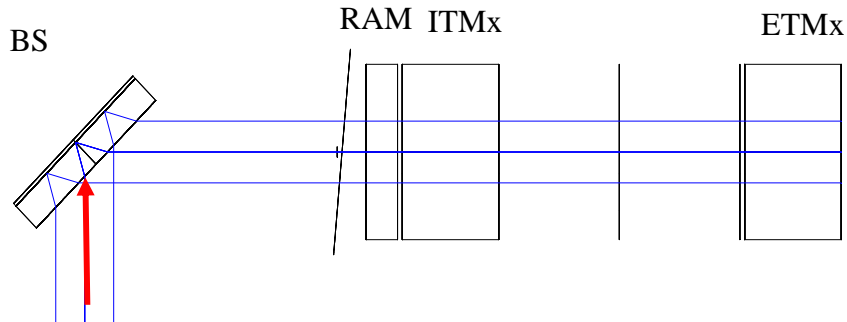


Figure 15: Optical Schematic, Signal Recycling Input Reflection from BS 50:50 Surface

3.1.3.1.1 Beam Cross-section at HR surface of ITMx

The x (vertical) and y (horizontal) beam cross sections at a location immediately behind the ITMx are shown in Figure 16 and Figure 17 respectively. Note that the y beam cross section is vignettted by a greater amount than the vertical beam cross section because of the tilted BS; the vignetting is symmetric because the input beam was translated to the optimal position.

The geometric power loss from traversing through the BS is $5.51E-5$ W.

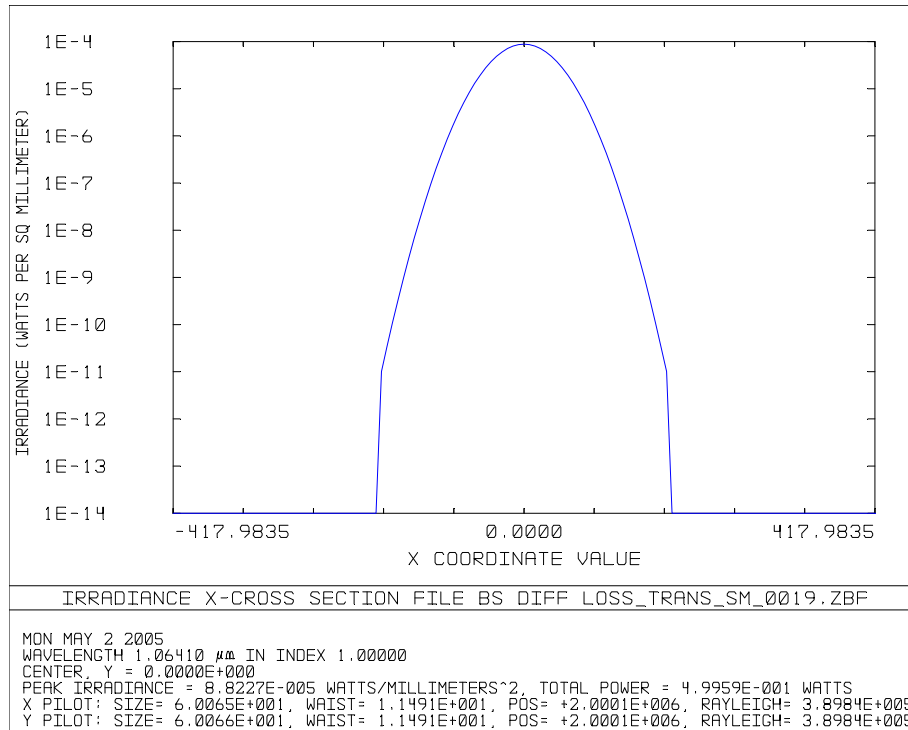


Figure 16: X-cross Section at ITMx HR, SR Input, Transmitted Arm

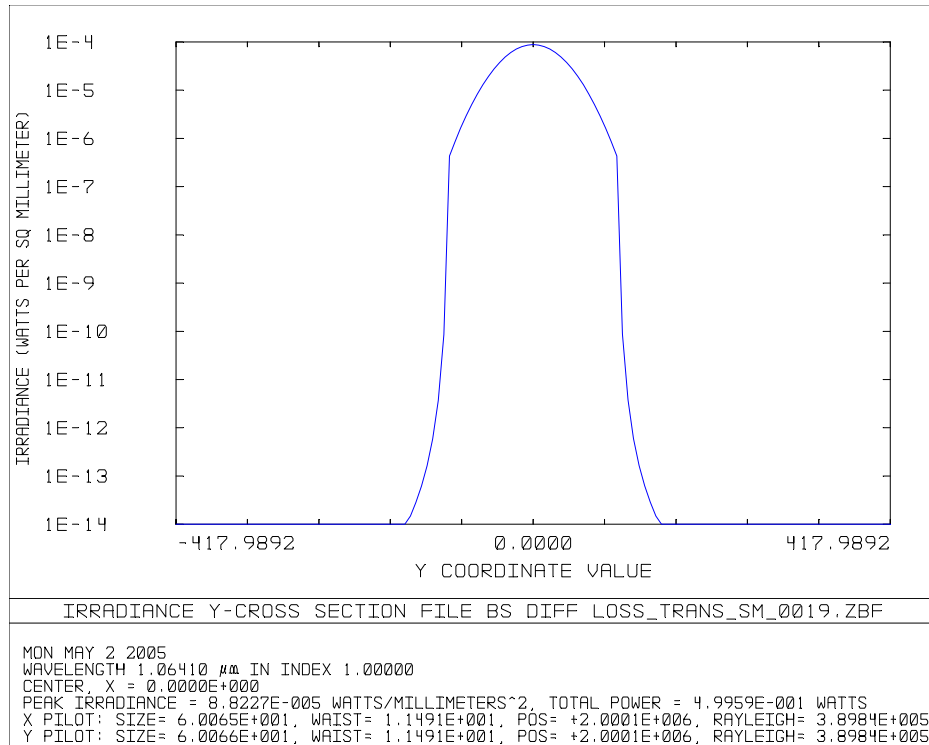


Figure 17: Y-cross Section at ITMx HR, SR Input, Transmitted Arm

3.1.3.1.2 Diffracted Power Loss around ETMx

The vignetted beam exhibits edge diffraction around the edges of the BS and the ITM. The diffracted beam is lost around the edges of the ETM, as shown in Figure 18 and Figure 19. Note that the lost diffracted power is greater in the y cross section.

The diffractive power loss at the ETMx is $1.10\text{E-}4$ W, approximately 25% of the geometric loss.

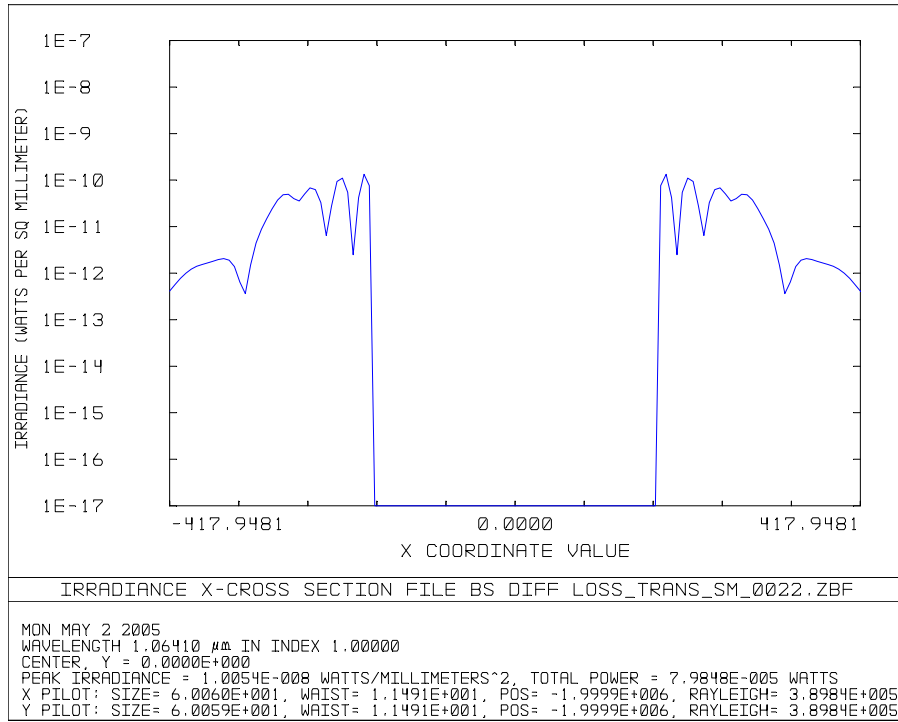


Figure 18: X-cross Section of Diffracted Beam around ETMx, SR Input, Transmitted Arm

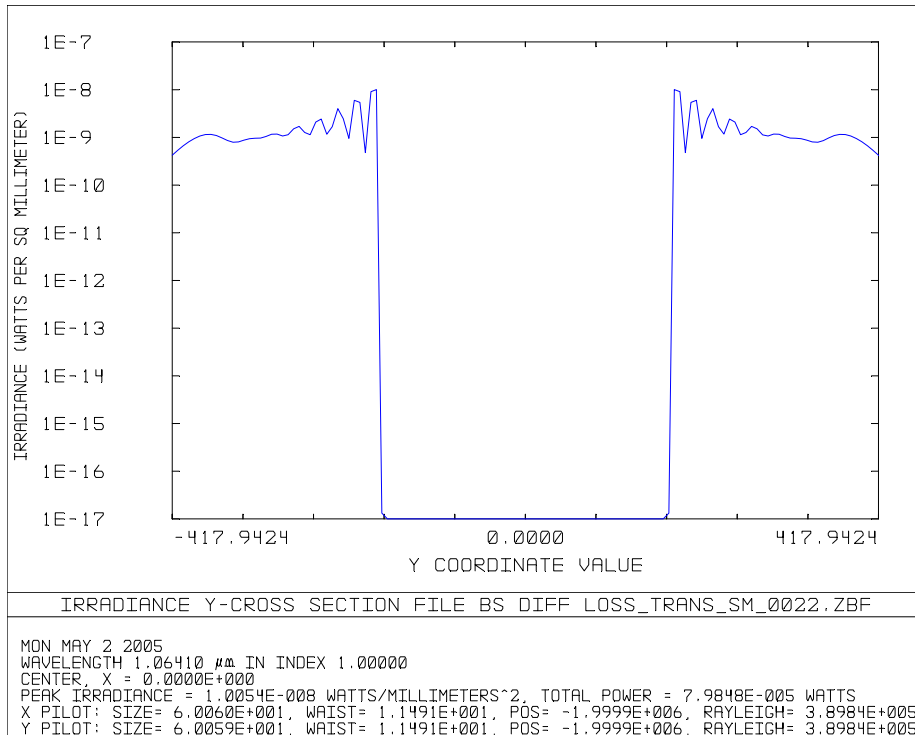


Figure 19: Y-cross Section of Beam around ETMx, SR Input, Transmitted Arm

3.1.3.2 Reflected Arm

An optical schematic of the reflected arm beam path with input from the signal recycling mirror (SR), transmitting through the BS, through the RAM, through the ITMy, and out to the ETMy is shown in Figure 20.

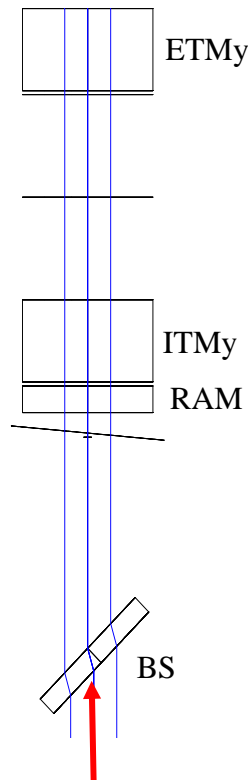


Figure 20: Optical Schematic, Signal Recycling Input Transmission through BS 50:50 Surface

3.1.3.2.1 Beam Cross-section at HR surface of ITMy, Reflected Arm

The x (vertical) and y (horizontal) beam cross sections at a location immediately behind the ITMy are shown in Figure 21 and Figure 22 respectively. Note that the y beam cross section is vignetted by a greater amount than the vertical beam cross section because of the tilted BS and is non-symmetrical because of the displacement of the beam at the BS AR surface.

The geometric power loss after traversing through the BS is $2.92\text{E-}4$ W.

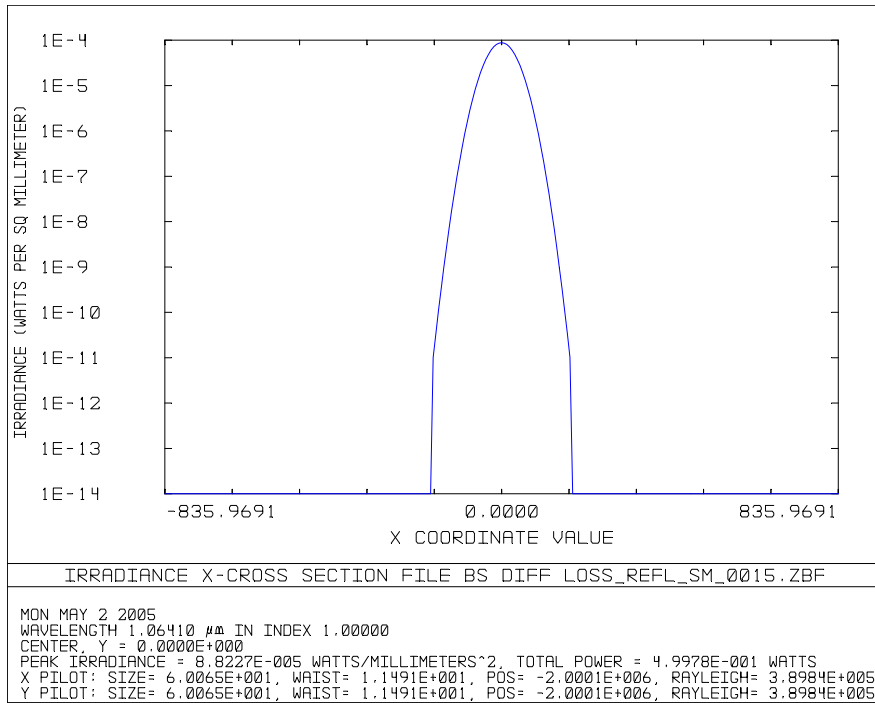


Figure 21: X-cross Section at ITMy HR, SR Input, Reflected Arm

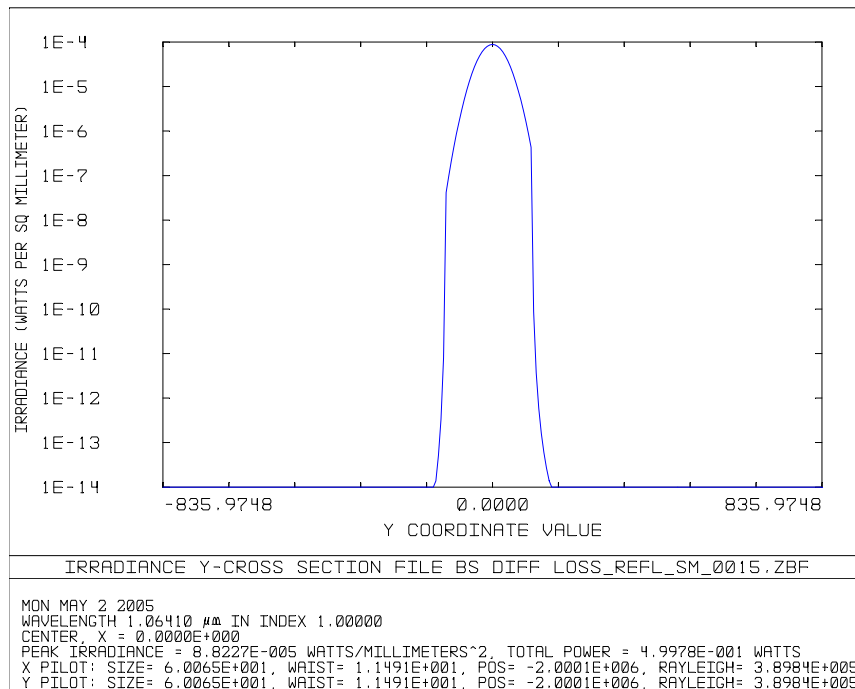


Figure 22: Y-cross Section at ITMy HR, SR Input, Reflected Arm

3.1.3.2.2 Diffracted Power Loss around ETMy

The vignetted beam exhibits edge diffraction around the edges of the BS and the ITM. The diffracted beam is lost around the edges of the ETM, as shown in Figure 23 and Figure 24. Note that the lost diffracted power is greater in the y cross section.

The diffractive power loss at the ETMy is $6.00E-5$ W, approximately 21% of the geometric loss.

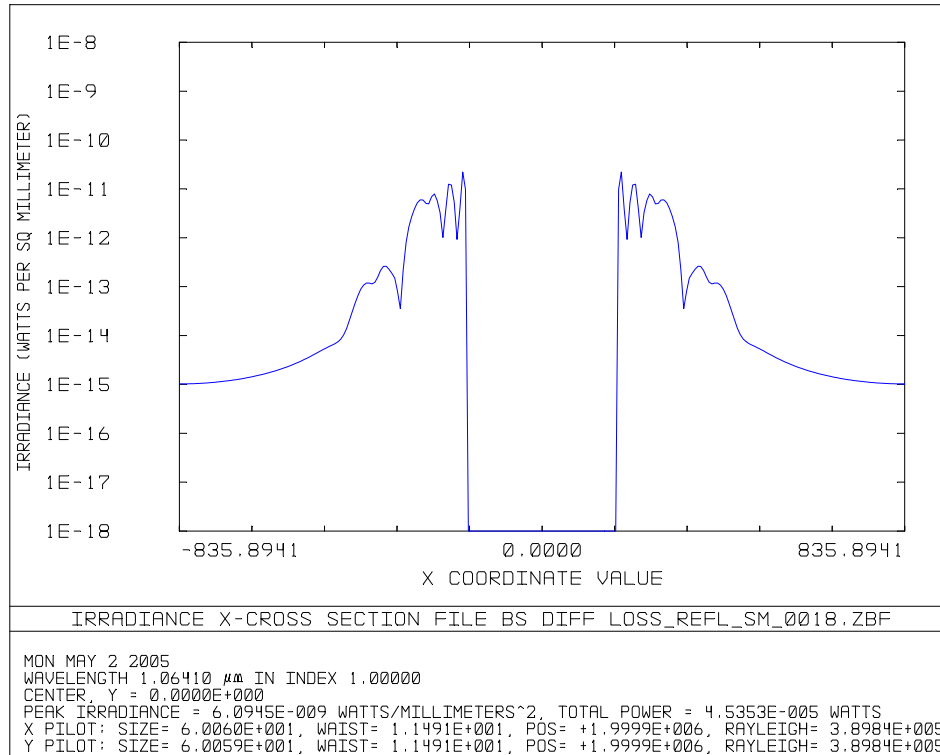


Figure 23: X-cross Section of Diffracted Beam around ETMy, SR Input, Reflected Arm

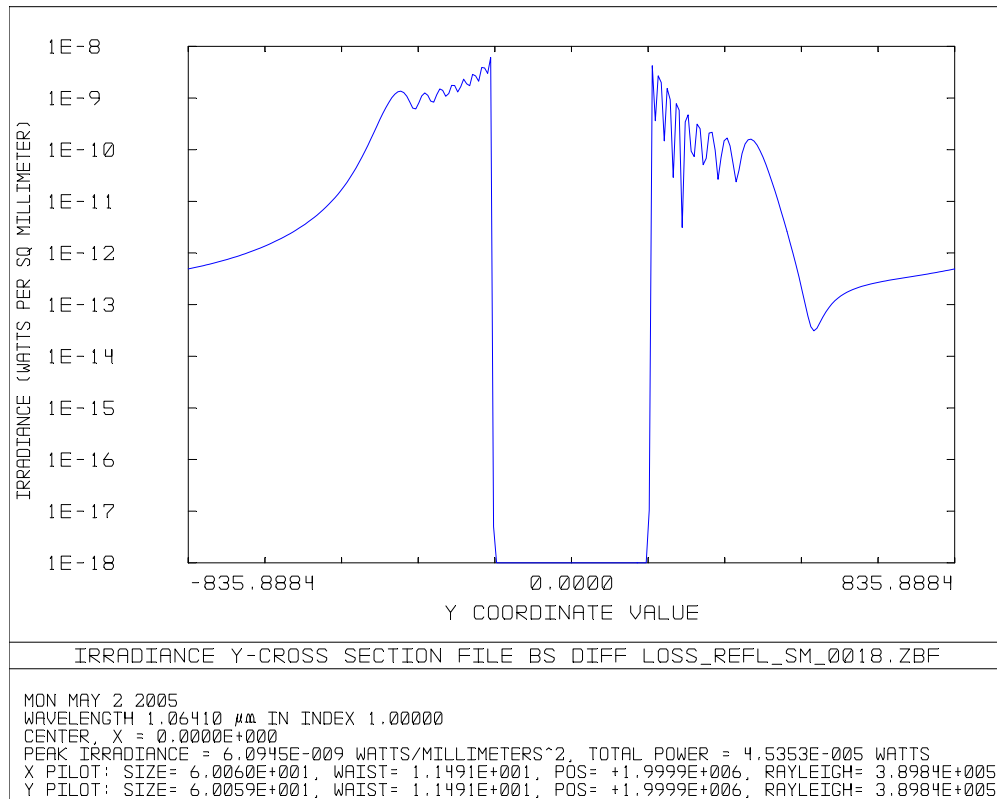


Figure 24: Y-cross Section of Diffracted Beam around ETMy, SR Input, Reflected Arm

The combined geometric and diffractive loss for both arms with SR input is $1.01\text{E}-3$ W.

3.1.4 Loss as a Function of BS Thickness and Diameter, No Bonding Flats

The geometric and diffractive power losses were calculated for a range of BS thicknesses between 50 mm to 72 mm, and a range of diameters between 350 mm to 400 mm. The calculations were performed for each arm separately with the beam input from the power recycling mirror (PR) and from the signal recycling mirror (SR). The results are shown in the following figures (loss in Watts with a 1 W input through the SR and PR mirrors).

3.1.4.1 Input Beam through Power Recycling Mirror, No Bonding Flats

3.1.4.1.1 Transmitted Arm Loss, PR Input

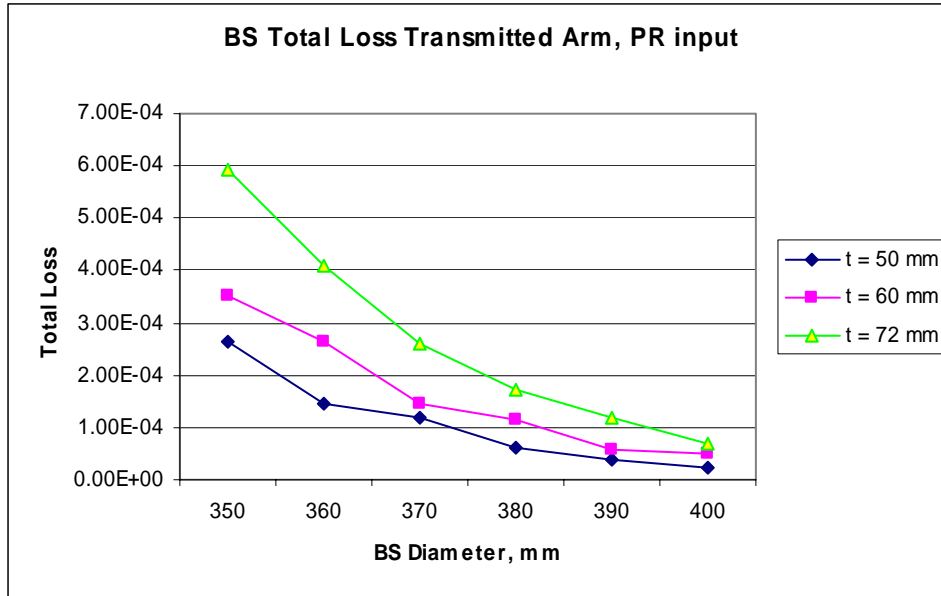


Figure 25: BS Total Loss Transmitted arm, PR Input

3.1.4.1.2 Reflected Arm Loss, PR Input

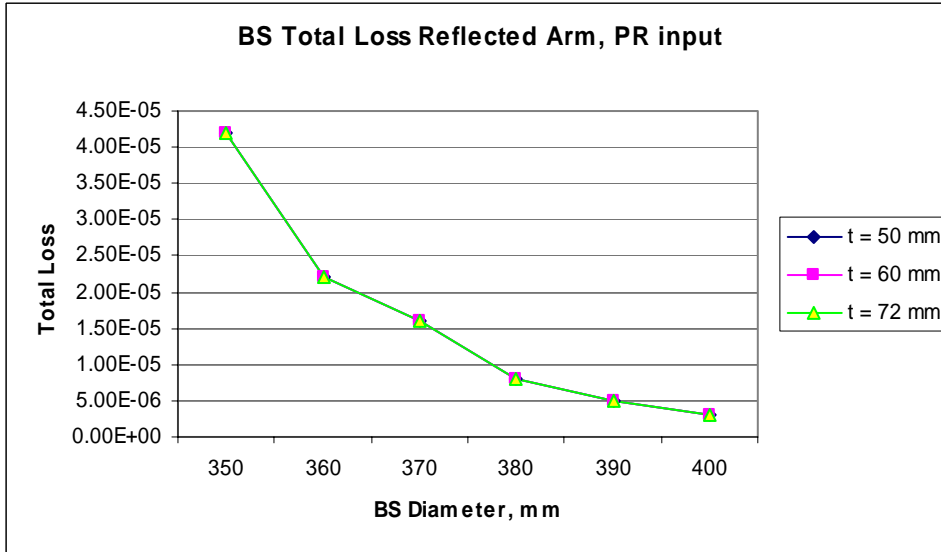


Figure 26: BS Total Loss Reflected arm, PR Input

3.1.4.1.3 Combined Loss, Both Arms, PR Input

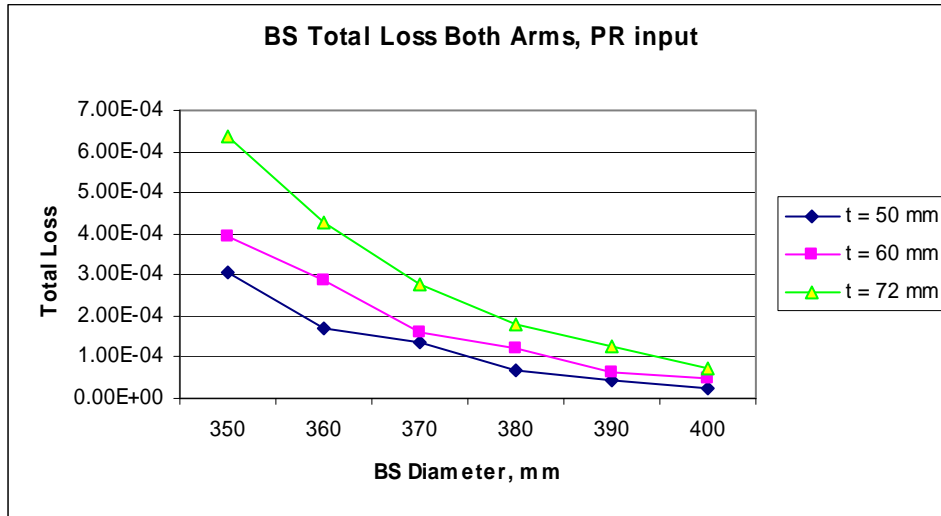


Figure 27: BS Total Loss Both Arms, PR Input

3.1.4.2 Input Beam through Signal Recycling Mirror, No Bonding Flats

3.1.4.2.1 Transmitted Arm Loss, SR Input

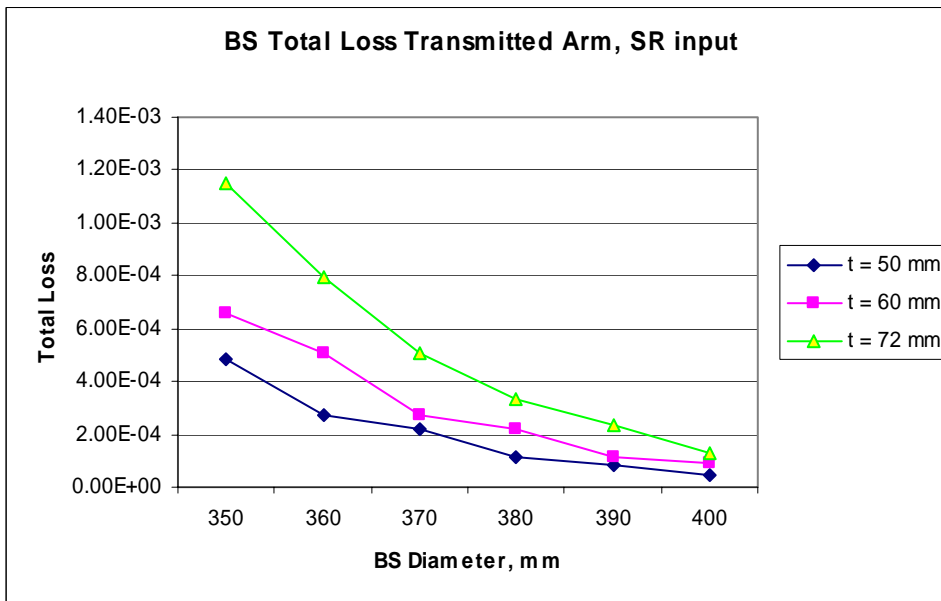


Figure 28: BS Total Loss Transmitted Arm, SR Input

3.1.4.2.2 Reflected Arm Loss, SR Input

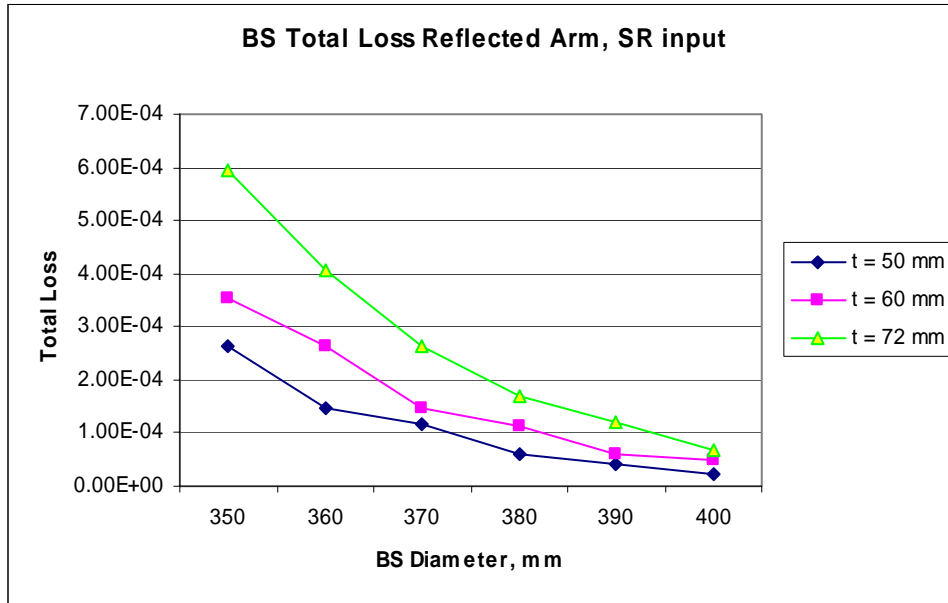


Figure 29: BS Total Loss Reflected Arm, SR Input

3.1.4.2.3 Combined Loss, Both Arms, SR Input

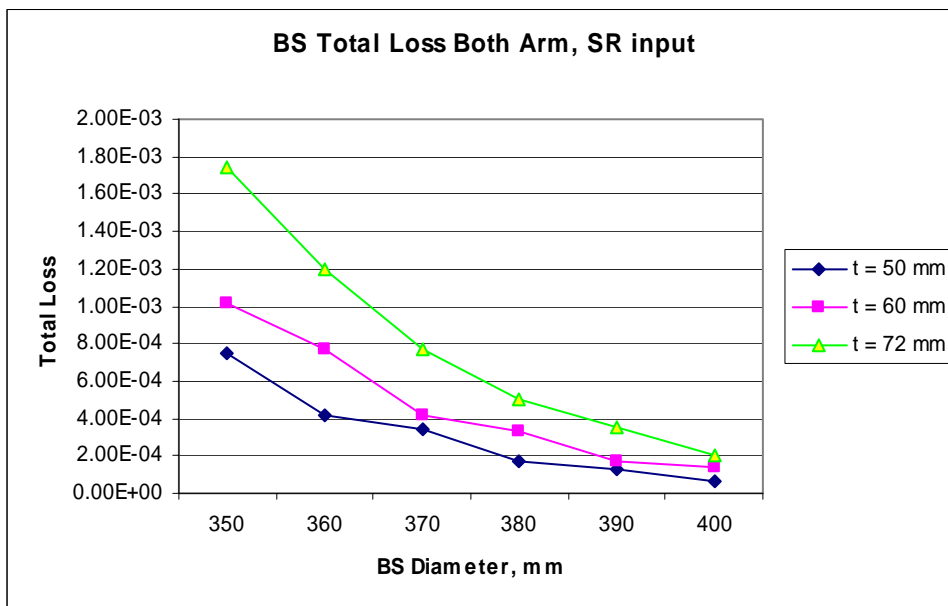


Figure 30: BS Total Loss Both Arms, SR Input

3.1.5 Loss as a Function of Bonding Flat Length

The combined geometric and diffraction losses (loss in Watts with a 1 W input through the SR and PR mirrors) from the placement of bonding flats on the vertical edges of the BS are shown in Figure 32 through Figure 37. The non-smooth data points are due to the finite sampling grid used by ZEMAX. The BS dimensions were taken to be $D = 370$ mm, and $t = 60$ mm.

3.1.5.1 Bonding Flat Geometry

The bonding flats on the BS were modeled in ZEMAX by placing a rectangular aperture next to the BS surface, as shown in Figure 31.

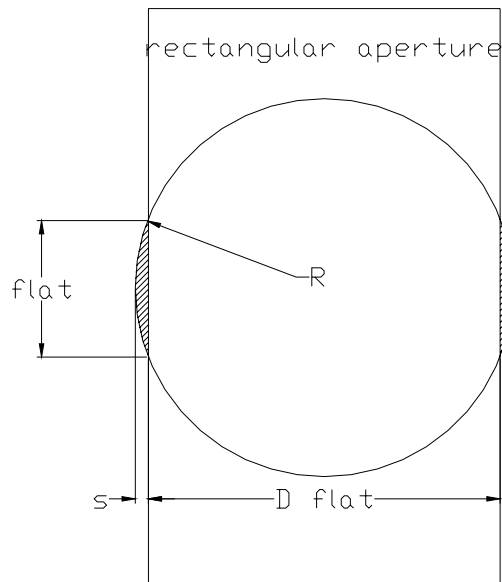


Figure 31: Bonding Flat Geometry

The sag required to produce a certain length of flat surface can be calculated from the following formula:

$$s = (flat/2)^2/2R$$

A 6.1 mm sag will produce a 95 mm flat length.

3.1.5.2 Input Beam through Signal Recycling Mirror (SR), with Bonding Flats

The total loss from both arms with SR input for various flat lengths is shown in Figure 34.

3.1.5.2.1 Loss in Transmitted Arm with Bonding Flat, SR Input

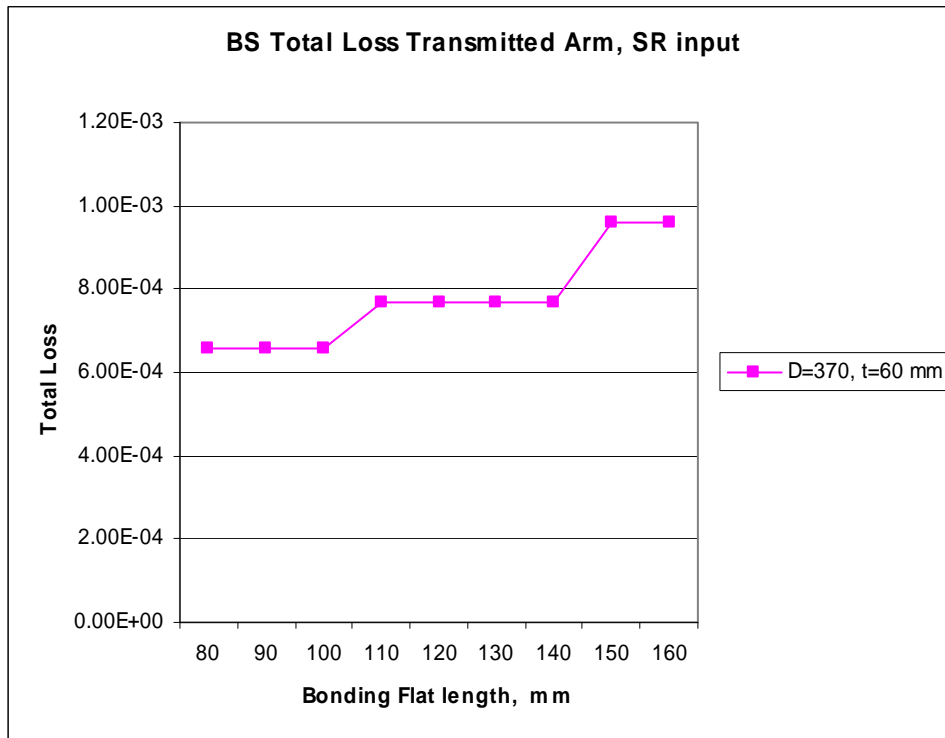


Figure 32: Power Loss in Transmitted Arm, SR Input with Flats

3.1.5.2.2 Loss in Reflected Arm with Bonding Flat, SR Input

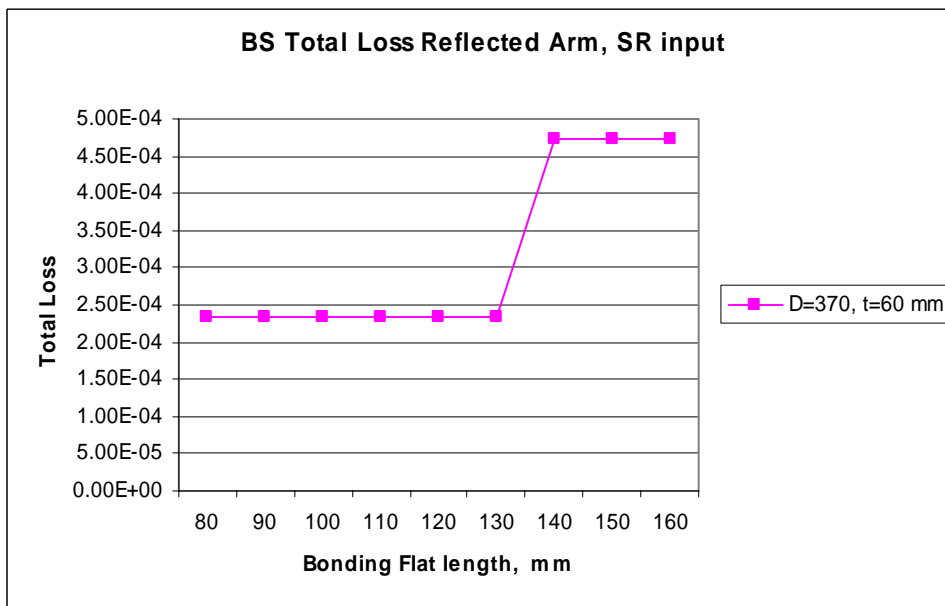


Figure 33: Power Loss in Reflected Arm, SR Input with Flats

3.1.5.2.3 Loss in Both Arms with Bonding Flat, SR Input

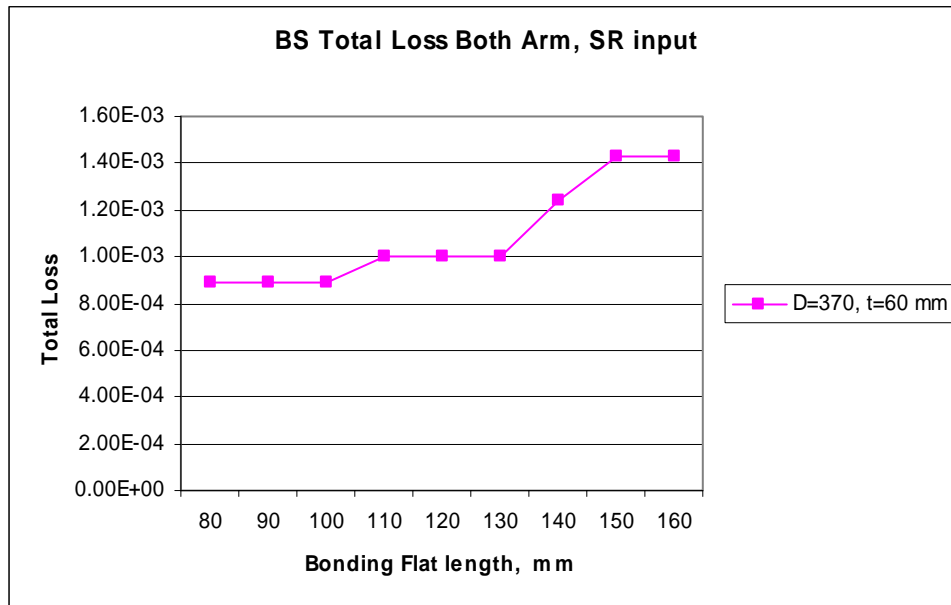


Figure 34: Power Loss in Both Arms, SR Input with Flats

3.1.5.3 Input Beam through Power Recycling Mirror (PR), with Bonding Flats

The total loss from both arms with PR input for various flat lengths is shown in Figure 37.

3.1.5.3.1 Loss in Transmitted Arm with Bonding Flat, PR Input

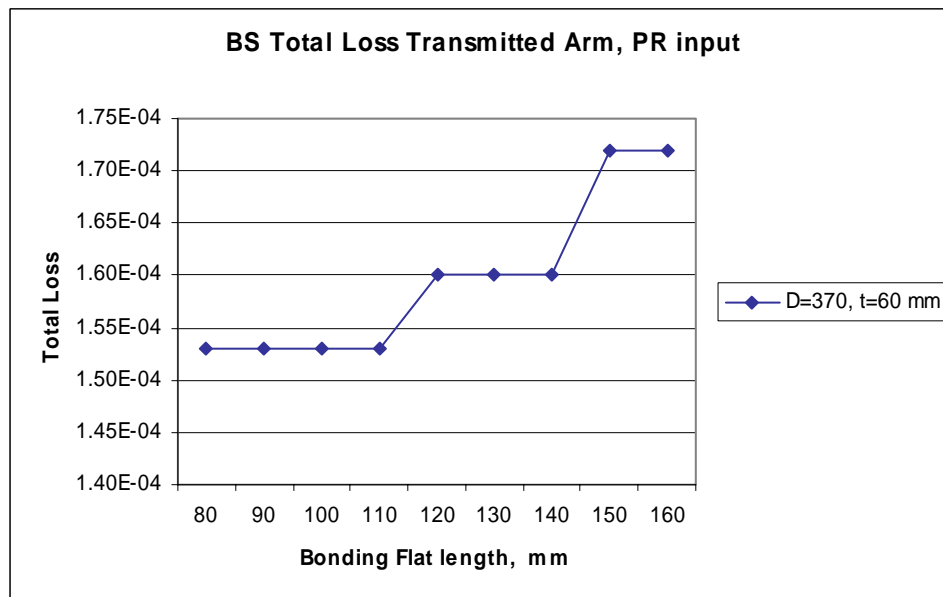


Figure 35: Power Loss in Transmitted Arm, PR Input with Flats

3.1.5.3.2 Loss in Reflected Arm with Bonding Flat, PR Input

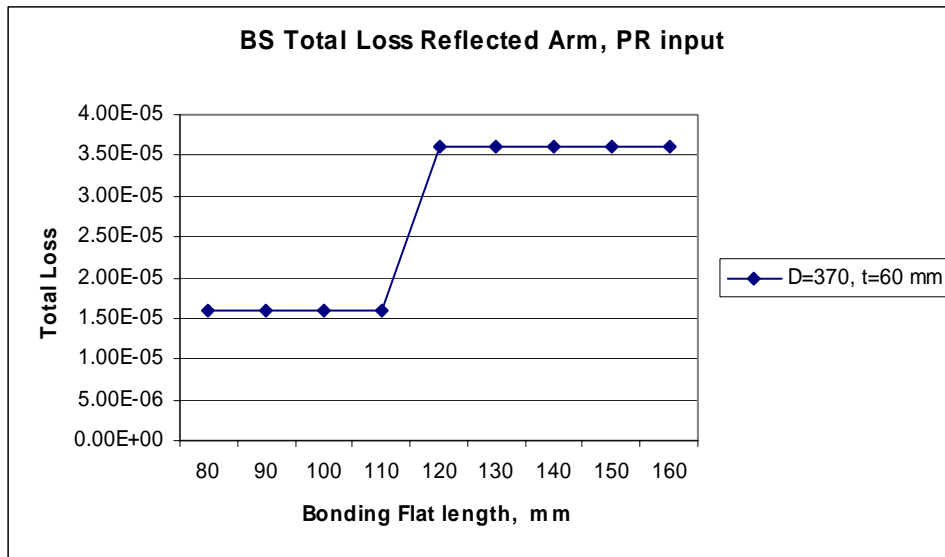


Figure 36: Power Loss in Reflected Arm, PR Input with Flats

3.1.5.3.3 Loss in Both Arms with Bonding Flat, PR Input

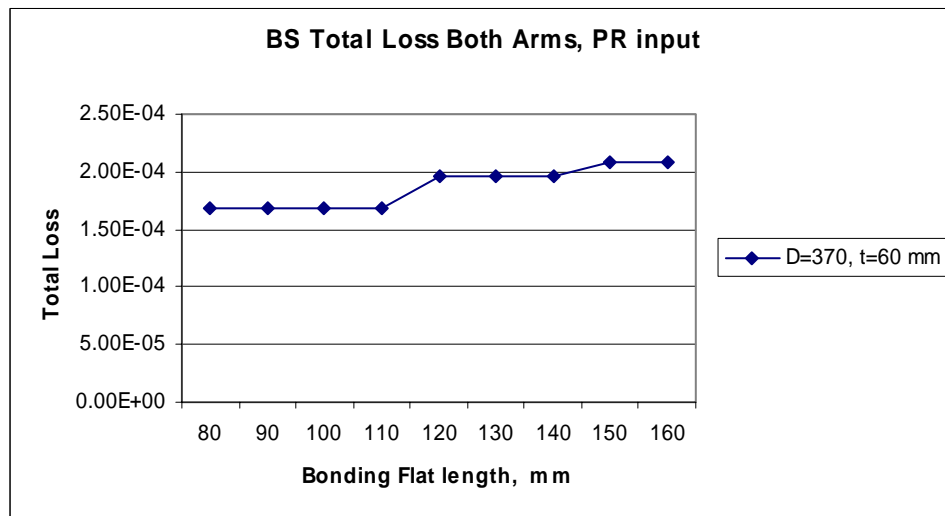


Figure 37: Power Loss in Both Arms, PR Input with Flats

3.2 Alternative Design with Lens at RAM

3.2.1 RAM Lens Configuration

The spot size at the BS is reduced from 60mm to 46.8 mm by placing a 9000 mm radius of curvature on the back surface of the reaction mass (RAM), as shown schematically in **Figure 38**.

This smaller spot size allows a significant reduction in the diameter of the BS for the same total power loss.

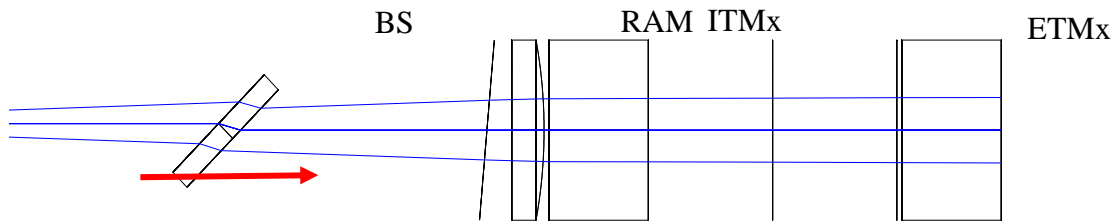


Figure 38: Optical Schematic, Alternative Design with Lens in RAM

The power losses, in Watts, from the BS with a 1 W input through the SR and PR mirrors are shown in Figure 39 through Figure 44.

3.2.2 BS Power Loss with RAM Lens

3.2.2.1 Input Beam through Power Recycling Mirror, RAM Lens

3.2.2.1.1 Transmitted Arm Loss, PR Input, RAM Lens

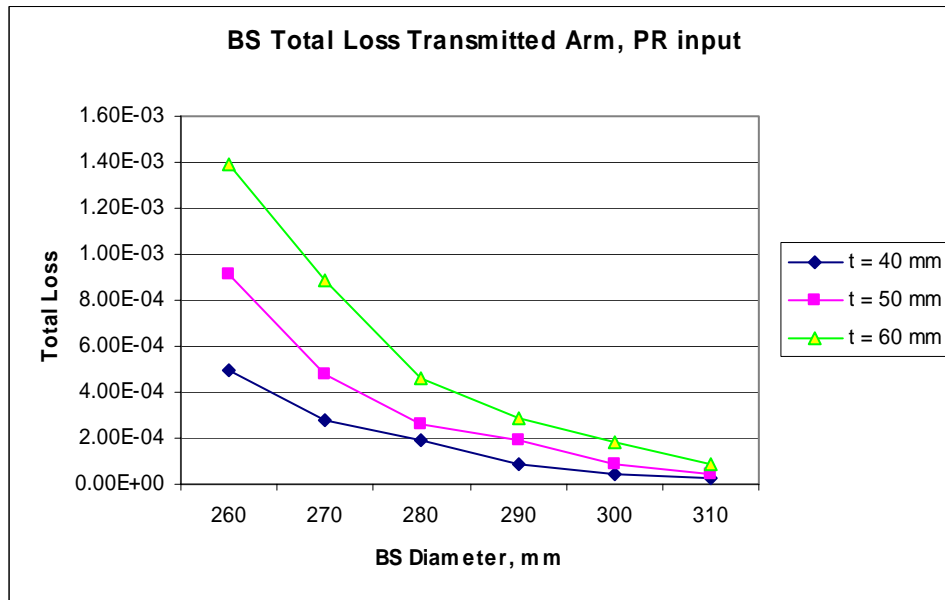


Figure 39: BS Total Loss Transmitted arm, PR Input with RAM lens

3.2.2.1.2 Reflected Arm Loss, PR Input, RAM Lens

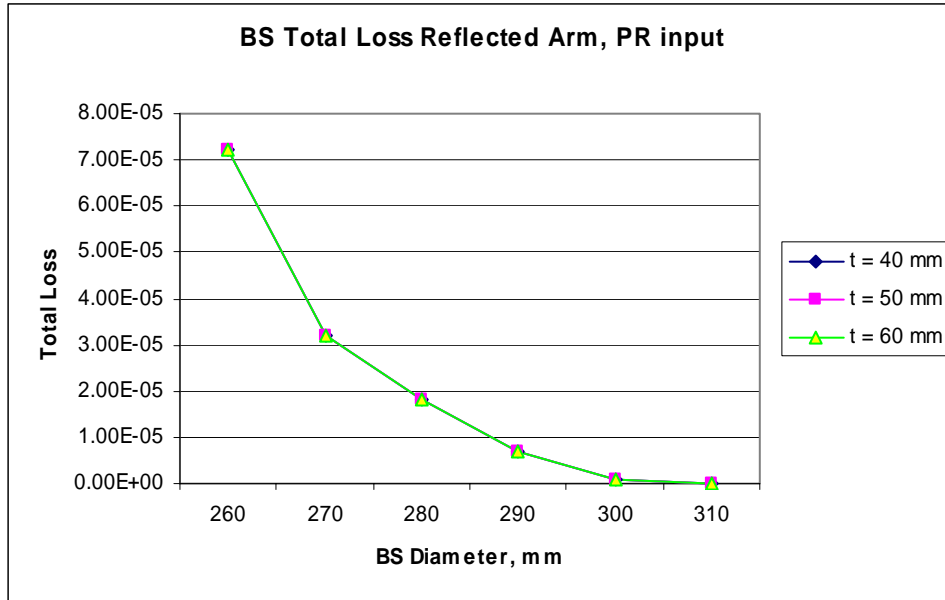


Figure 40: BS Total Loss Reflected arm, PR Input with RAM lens

3.2.2.1.3 Combined Loss, Both Arms, PR Input, RAM Lens

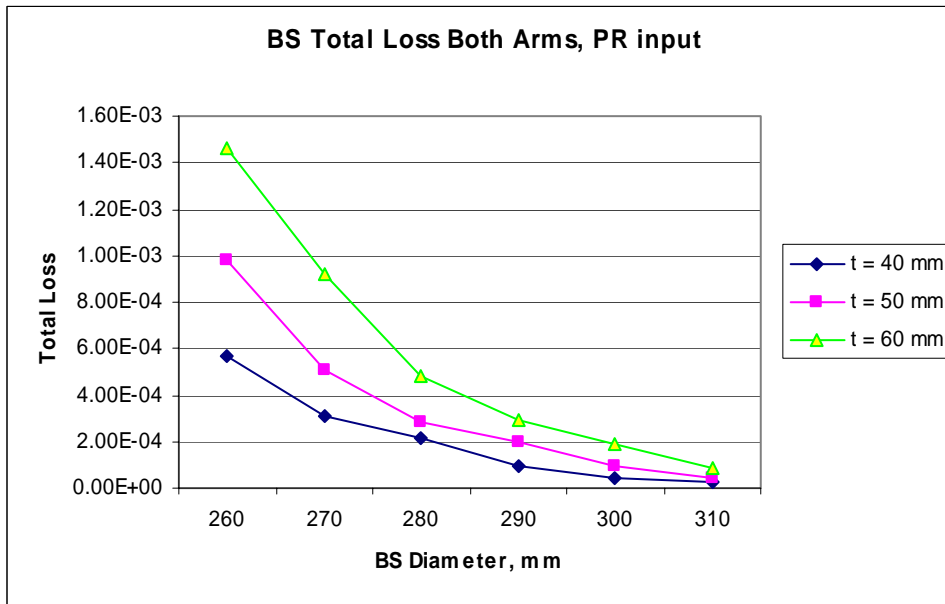


Figure 41: BS Total Loss Both Arms, PR Input with RAM lens

3.2.2.2 Input Beam through Signal Recycling Mirror, RAM Lens

3.2.2.2.1 Transmitted Arm Loss, SR Input, RAM Lens

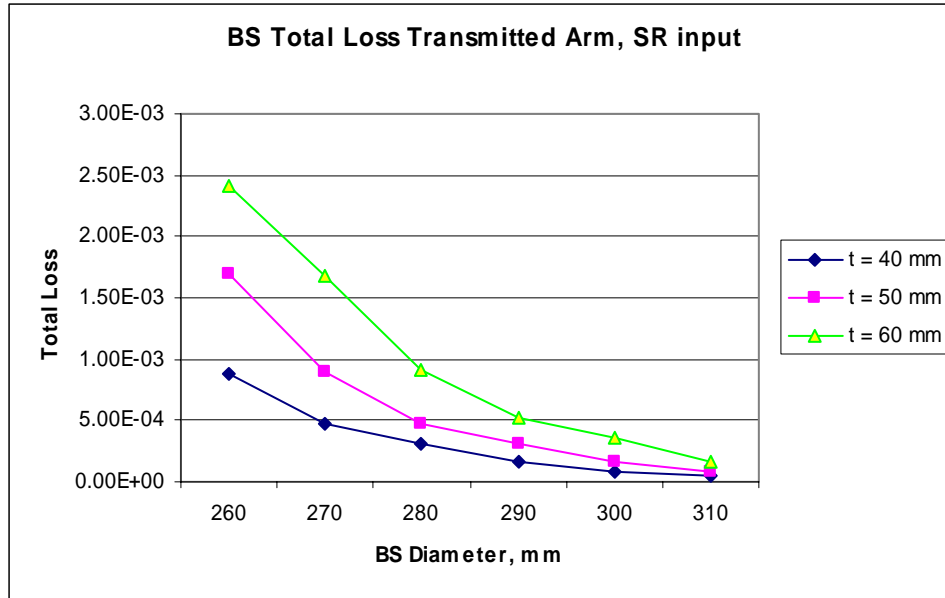


Figure 42: BS Total Loss Transmitted Arm, SR Input with RAM lens

3.2.2.2.2 Reflected Arm Loss, SR Input, RAM Lens

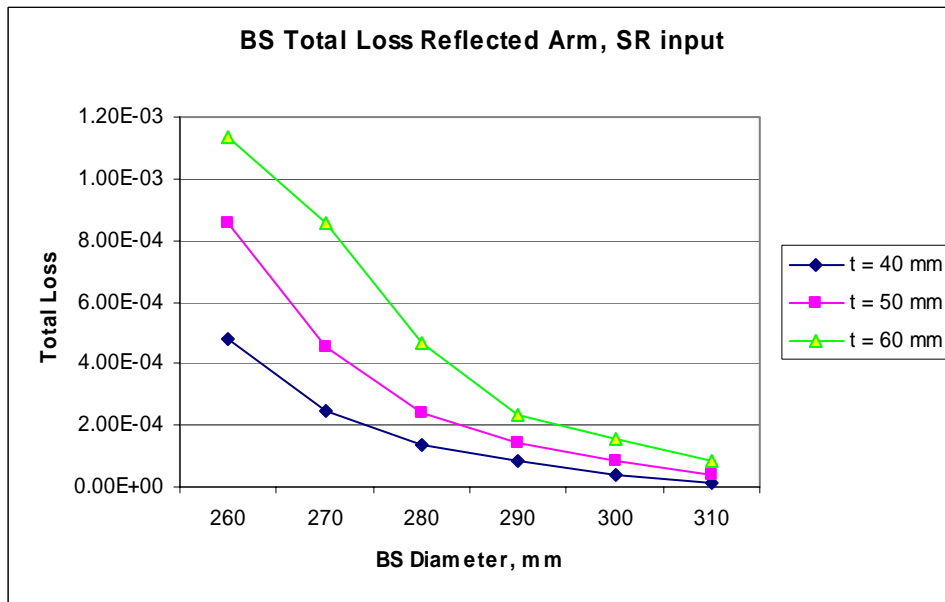


Figure 43: BS Total Loss Reflected Arm, SR Input with RAM lens

3.2.2.2.3 Combined Loss, Both Arms, SR Input, RAM Lens

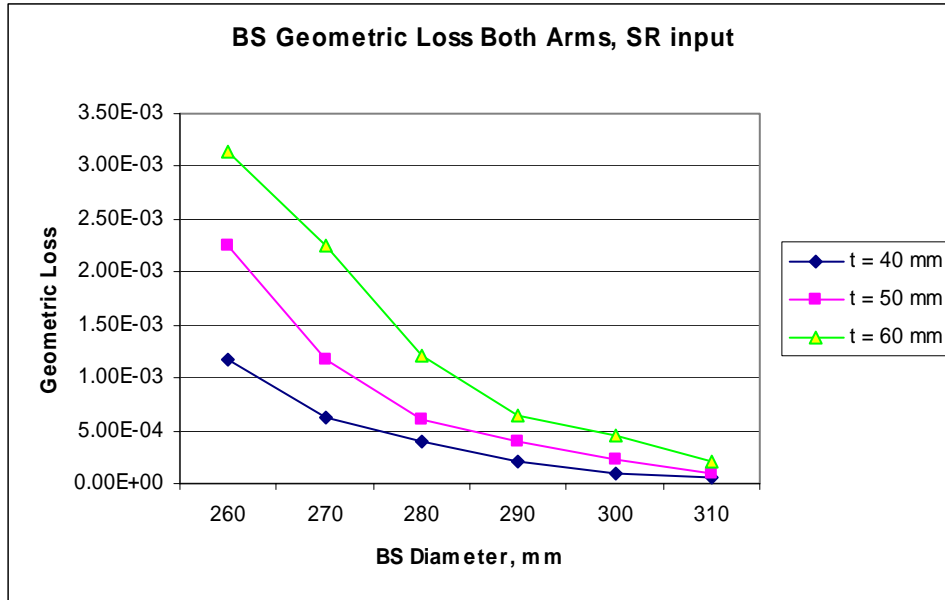


Figure 44: BS Total Loss Both Arms, SR Input with RAM lens

3.2.3 Beam Steering with RAM Lens

Placing a lens element at the RAM causes a lateral displacement of the beam through the RAM lens to steer the beam at the ETM, as shown in Figure 45.

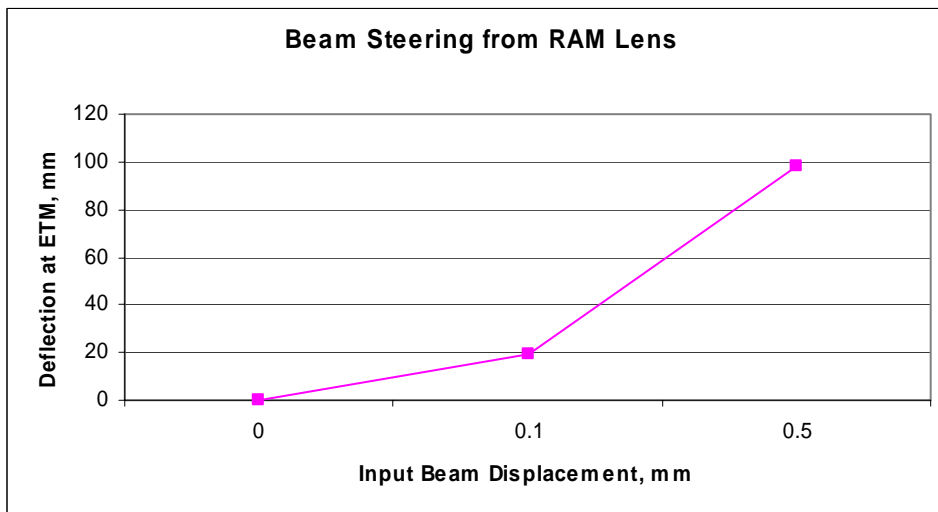


Figure 45: Beam Steering by RAM Lens

4 Conclusions

The geometric loss due to vignetting of the beam at the tilted BS surface accounts for more than 75% of the total power loss of the input beam.

The loss of the input beam from the SR mirror is approximately 2.5 times larger than the loss of the input beam from the PR mirror.

Centering the input beam from the PR mirror minimizes the total optical loss from both recycling mirror directions.

4.1 Standard Configuration: No Lensing at RAM

Table 1 summarizes the total geometric loss and diffractive losses from the two recycling mirror directions in making one traversal to the ETM for two possible BS dimensions, one of which is the Adv LIGO baseline configuration ($t = 60\text{mm}$, $D = 350\text{ mm}$).

The diameter/thickness ratio (D/t) is also shown. For reference, the D/t ratio for the Initial LIGO BS is 6.25. The D/t ratio may affect the coating-induced sag of the BS HR surface.

The second configuration, with $t = 60\text{ mm}$, $D = 370\text{ mm}$ has a diffractive loss 2.4 times smaller than the baseline and has a $D/t = 6.2$ that is comparable to the Initial LIGO configuration.

Table 1 : BS Loss Comparison for Two Configurations

BS DIMENSIONS	PR LOSS BOTH ARMS	SR LOSS BOTH ARMS	D/t
$t = 60\text{mm}$, $D = 350\text{ mm}$	3.94 E-4	1.01 E-3	5.8
$t = 60\text{mm}$, $D = 370\text{ mm}$	1.61 E-4	4.18 E-4	6.2

4.2 Alternate Configuration: 9000 mm Radius on Back Surface of RAM

Table 2 summarizes the total geometric loss and diffractive losses from the two recycling mirror directions in making one traversal to the ETM for two possible alternative BS dimensions.

The diameter/thickness ratio (D/t) is also shown.

The second configuration, with $t = 50\text{ mm}$, $D = 300\text{ mm}$ has a total loss 5.6 times smaller than the first configuration.

Table 2: Alternative Design, BS Loss Comparison for Two Configurations

BS DIMENSIONS	PR LOSS BOTH ARMS	SR LOSS BOTH ARMS	D/t
$t = 40\text{mm}$, $D = 260\text{ mm}$	5.69 E-4	1.18 E-3	6.5
$t = 50\text{mm}$, $D = 300\text{ mm}$	9.10 E-5	2.18 E-04	6.0

4.2.1 Potential Problems with Lens at RAM

The significant beam steering caused by the RAM lens may place a severe restriction on the available positioning range of the beam at the ITM. A 0.5 mm displacement of the beam at the ITM results in a 100 mm displacement at the ETM.

Additionally, the non-parallel rays at the BS may cause astigmatism of the input and output beams.

4.3 Power Loss Due to Bonding Flats

With a BS size of $t = 60\text{mm}$ and $D = 370\text{ mm}$, bonding flats up to 100 mm long result in a total power loss in both arms of less than 0.1%. E.g. the power loss with SR input of 1 W is 9 E-4 W , and with PR input of 1 W is 1.7 E-4 W .